scientific reports

Check for updates

OPEN

The brain prioritizes the basic level of object category abstraction

Michelle R. Greene[1,2]✉ & Alyssa Magill Rohan[1,3]

The same object can be described at multiple levels of abstraction ("parka", "coat", "clothing"), yet human observers consistently name objects at a mid-level of specificity known as the basic level. Little is known about the temporal dynamics involved in retrieving neural representations that prioritize the basic level, nor how these dynamics change with evolving task demands. In this study, observers viewed 1080 objects arranged in a three-tier category taxonomy while 64-channel EEG was recorded. Observers performed a categorical one-back task in different recording sessions on the basic or subordinate levels. We used time-resolved multiple regression to assess the utility of superordinate-, basic-, and subordinate-level categories across the scalp. We found robust use of basic-level category information starting at about 50 ms after stimulus onset and moving from posterior electrodes (149 ms) through lateral (261 ms) to anterior sites (332 ms). Task differences were not evident in the first 200 ms of processing but were observed between 200–300 ms after stimulus presentation. Together, this work demonstrates that the object category representations prioritize the basic level and do so relatively early, congruent with results that show that basic-level categorization is an automatic and obligatory process.

Keywords Object categorization, Temporal dynamics, Task demands, EEG

Object recognition is a ubiquitous human activity that we find fast and effortless[1]. Every act of object recognition is also an act of categorization[2]. For example, to recognize the coffee cup on one's desk, one places it into the class of *coffee cups*, thus linking it to the knowledge we have about the concept as a whole (holds hot liquid, often has a handle, is smaller than a breadbox, etc.) Thus, categorization is also an act of cognitive information compression that enables us to act efficiently and intelligibly[3].

Each object can be categorized with multiple valid labels because the human conceptual structure is hierarchical[4]. For example, the same coffee cup could be a "cup", a "dish", an "object", or an "entity" with increasing levels of abstraction, or a "black coffee cup from a 2017 conference" at a more specific level. Yet, observers tend to use some labels more often than others[5]. Specifically, most objects are spontaneously named at a mid-level of specificity known as the "basic"[6]or "entry"[7]level. The salience of this category level has been established with developmental, cognitive, and cognitive neuroscience studies. Children's language is composed primarily of basic-level names[6,8,9]. For adults, objects are categorized fastest at the basic level[6,10,11]. Basic-level words also tend to be shorter[5,6], highlighting how using basic-level terms provides efficient communication.

While the salience of the basic level is well-established in cognitive literature, comparatively few studies have examined the neural correlates of this effect. Object recognition is believed to involve a series of regions in the ventral visual processing stream[12]. Of particular note is the lateral occipital complex (LOC), an area with higher selectivity to intact objects than scrambled objects, faces, or scene[13]. However, studies employing multivoxel pattern analysis (MVPA) have demonstrated that object identities and categories can be decoded throughout the occipitotemporal cortex[14–18], suggesting that the neural code for object categories is broadly distributed across the cortex. Critically, many of the objects selected for these studies were chosen to widely sample objects as a natural class, with little respect to their hierarchical relationships. One counterexample[16] examined object decoding at three levels of specificity: superordinate (domain level), basic, and subordinate (the most specific level). This study found that although early visual cortex showed the best category clustering at the subordinate level (perhaps reflecting the higher low-level similarities among exemplars at this level), basic-level grouping increased across the ventral visual stream, with an observed maximum in LOC. An open question concerns the temporal dynamics of the basic level superiority effect. By knowing when the brain prioritizes basic-level categories, we can begin to infer how this prioritization occurs.

The temporal dynamics of object categorization are particularly critical, as this task is effortless[1,19–21]and may even be automatic, as we engage in categorization even when it is task-irrelevant[22,23]. Previous studies on the

[1]Bates College Program in Neuroscience, Bates College, Lewiston, ME, USA. [2]Department of Psychology, Barnard College, Columbia University, 3009 Broadway, New York NY 10027, USA. [3]Boston Children's Hospital, Boston, USA. ✉email: mgreene@barnard.edu

neural time course of object categorization have included a wide array of objects without a specific hierarchical relationship to one another[24–26], examined category relationships at a superordinate level, such as animate versus inanimate[27–30]or examined hierarchical relationships among objects in a post-hoc manner[31,32]. These previous studies on the temporal dynamics of object decoding have found that object exemplars can begin to be decoded around 60 ms after stimulus onset[27,33–35]. However, this performance may be enabled by differences in the low-level visual features associated with the images rather than the categories per se. Supporting evidence for this view is that decodable M/EEG signals of object exemplars correlate with behavioral assessments of similarity or reaction times later (150–250 ms after stimulus onset[21,25,36–38]). Furthermore, position and size-invariant decoding only occur after 135 ms[35,39]. Finally, studies that have examined abstract, category-level decoding versus exemplar-level decoding have found that neural signals do not contain object category information until around 250 ms after stimulus onset[28,33].

Despite the consistency of these findings, many questions about object category representation remain. Specifically, none of these previous decoding studies have examined categorization at the basic- or entry-level in comparison to other levels of abstraction. Furthermore, we have little insight into how the observer's task influences these temporal dynamics. Accordingly, this study was designed to examine hierarchical relationships among objects at three different levels of specificity. Moreover, as some superordinate-level distinctions such as animacy[40]or real-world size[41] may engage distinct neural pathways, we have chosen this stimulus set from a small number of superordinate-level categories that, as best as possible, are inanimate and large in size.

Our approach is illustrated in Fig. 1. We examined how three levels of object category information are reflected in time-resolved EEG responses when observers engaged in two different categorization tasks, a basic-level task, and a subordinate-level task. We focused on these two levels because the superordinate is the least important. Superordinate-level terms are used with the least frequency[42], and children learn superordinate-level terms last[6,43]. Furthermore, behavioral evidence has suggested that category membership at the superordinate level is inferred from the basic level, which is perceived directly[6,22,44]. Last, although expertise can shift the entry-level of an object from basic- to subordinate[11], there are no analogous experiences that shift the entry level to the superordinate within cognitively healthy individuals. Objects were selected from large, inanimate objects and pasted on an abstract background to avoid confounds from correlated natural backgrounds and previously established category distinctions. Multiple competing predictions can be made. If object categorization proceeds from low-level features to more abstract categories, as shown by[28,33], we expect the earliest neural responses to correspond to the subordinate-level category, followed by the basic and then the superordinate. However, if categorization proceeds in a top-down manner, we may expect the degree of shared semantic features[24,31,45]to be processed first. As superordinate-level categories would require the fewest number of semantic features to be verified to determine category membership, this would predict that superordinate-level categories would be read out first. Finally, given the behavioral importance of the basic level for categorization[6], the most rapid and robust neural responses may be at this level.

Results

Behavioral

In two sessions, observers detected category repeats at either the basic or subordinate levels. Overall, performance on the repeat detection task was high (mean: 94%, range: 86%−97%). We computed d' for both tasks and found that although performance was numerically higher on the basic-level task (mean: 2.67) than on the subordinate-level task (mean: 1.90), this difference was not statistically significant ($t(13) = 1.65$, $p = 0.12$). Therefore, participants were similarly successful on both tasks. We examined the detection rate across subordinate-level categories. We found it very high (mean: 94%, range: 91%−100%), indicating that observers could easily distinguish between all subordinate-level categories.

We also compared the reaction times for the hits of both tasks. We found that participants were faster at detecting basic-level repeats (mean: 798 ms) compared to subordinate-level repeats (mean: 846 ms, $t(13) = -3.56$, $p = 0.003$).

Whole-brain multiple regression

At each time point, we fit a multiple linear regression model using the lower triangle of the three orthogonalized model RDMs in Fig. 1B as predictors for the representational dissimilarity matrix of EEG responses across the 64 electrodes and 1080 trials. We stored the regression coefficients (β) and the coefficient of determination for the model (R^2). The results of the time-resolved R^2 analysis are shown in Fig. 2A. Overall, both basic-level (green) and subordinate-level (purple) detection tasks had very similar onsets (both 72 ms, $t(13) < 1$). Similarly, both tasks had identical maximum R^2 values (0.00012, $t(13) < 1$) and similar latencies of maximum R^2 (basic: 149 ms, subordinate: 153 ms, $t(13) < 1$). For each participant, we subtracted the R^2 for the subordinate task from the R^2 in the basic task. We confirmed that no significant task differences were observed at any time point (see Fig. 2B). Therefore, both tasks seem to engage category information similarly.

Next, we examined the regression coefficients for each of the three category models across both tasks. The results are shown in Fig. 2C. To examine the earliest use of category information, we performed a repeated measures ANOVA on the onset values with task and category models as within-subject variables. We found no significant effect of task (basic: 64 ms; subordinate: 49 ms, $F(1,13) < 1$). Although we found a numerical trend toward later onsets for the subordinate-level model (68 ms) compared to the basic (52 ms) and superordinate (50 ms) models, this difference did not achieve statistical significance ($F(2,26) < 1$). Finally, there was no significant interaction between task and category model ($F(2,26) < 1$) on the onset of regression coefficients.

We then considered the maximum coefficient values for each category model and task. We found a significant main effect of category model ($F(2,26) = 21.4$, $p < 0.001$, $ges = 0.99$). Post-hoc analyses revealed that this was driven by higher coefficient values for the basic-level category model than the subordinate (0.77 versus 0.27,

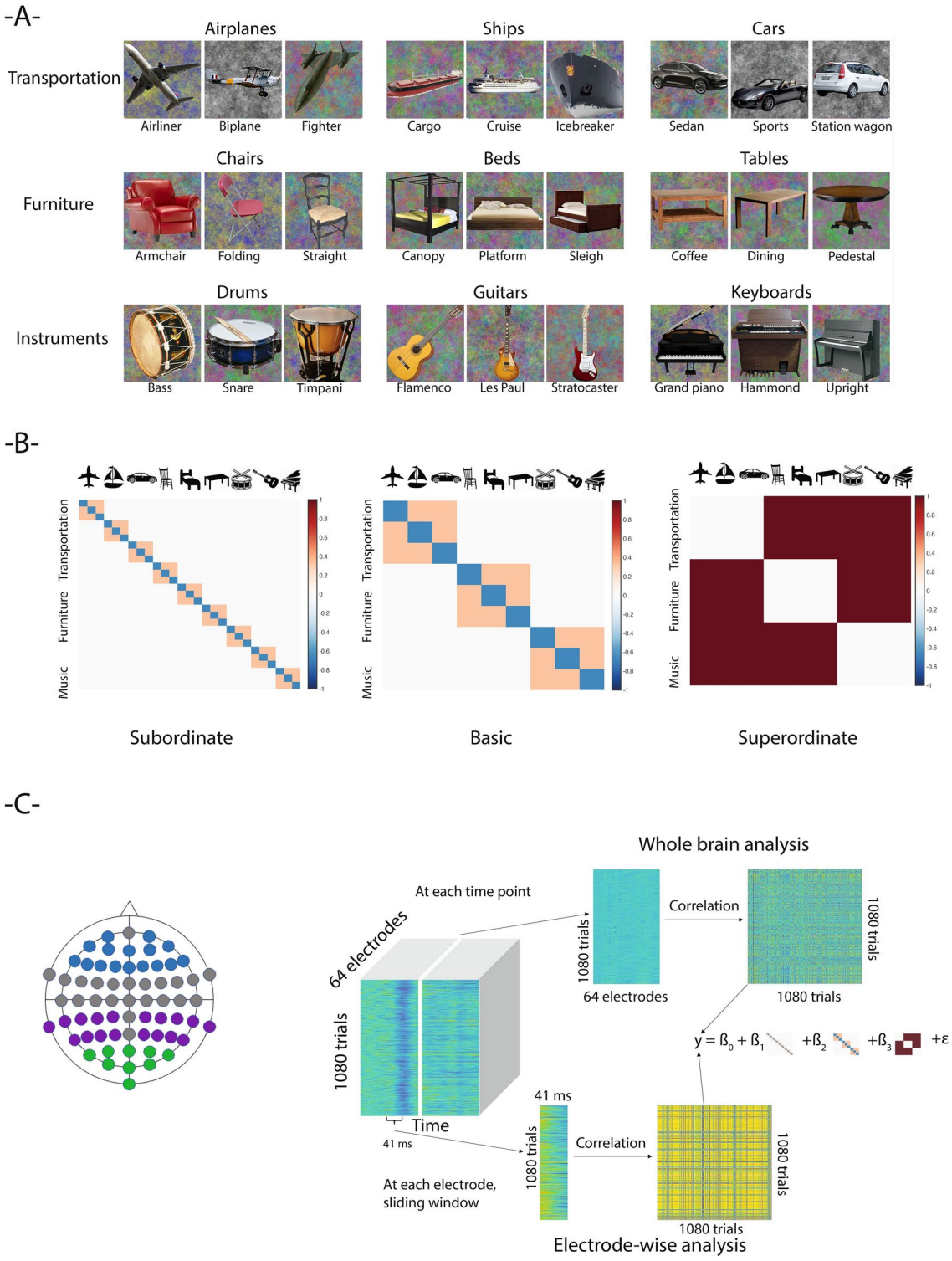

Fig. 1. (**A**) Example images of each of the 27 subordinate-level object categories. There were 40 exemplars in each of these categories. Please note that the names are written here for convenience and were not presented to the participants. (**B**) Representational dissimilarity matrices (RDMs) depict orthogonalized subordinate-, basic-, and superordinate-level models. (**C**) Illustration of multiple regression methods. The scalp map shows the three regions of interest (ROIs). The top pathway illustrates whole-brain regression while the bottom illustrates the electrode-wise approach. In both cases, the resulting neural representational dissimilarity matrices (RDMs) were predicted by the three model RDMs from panel **B**.

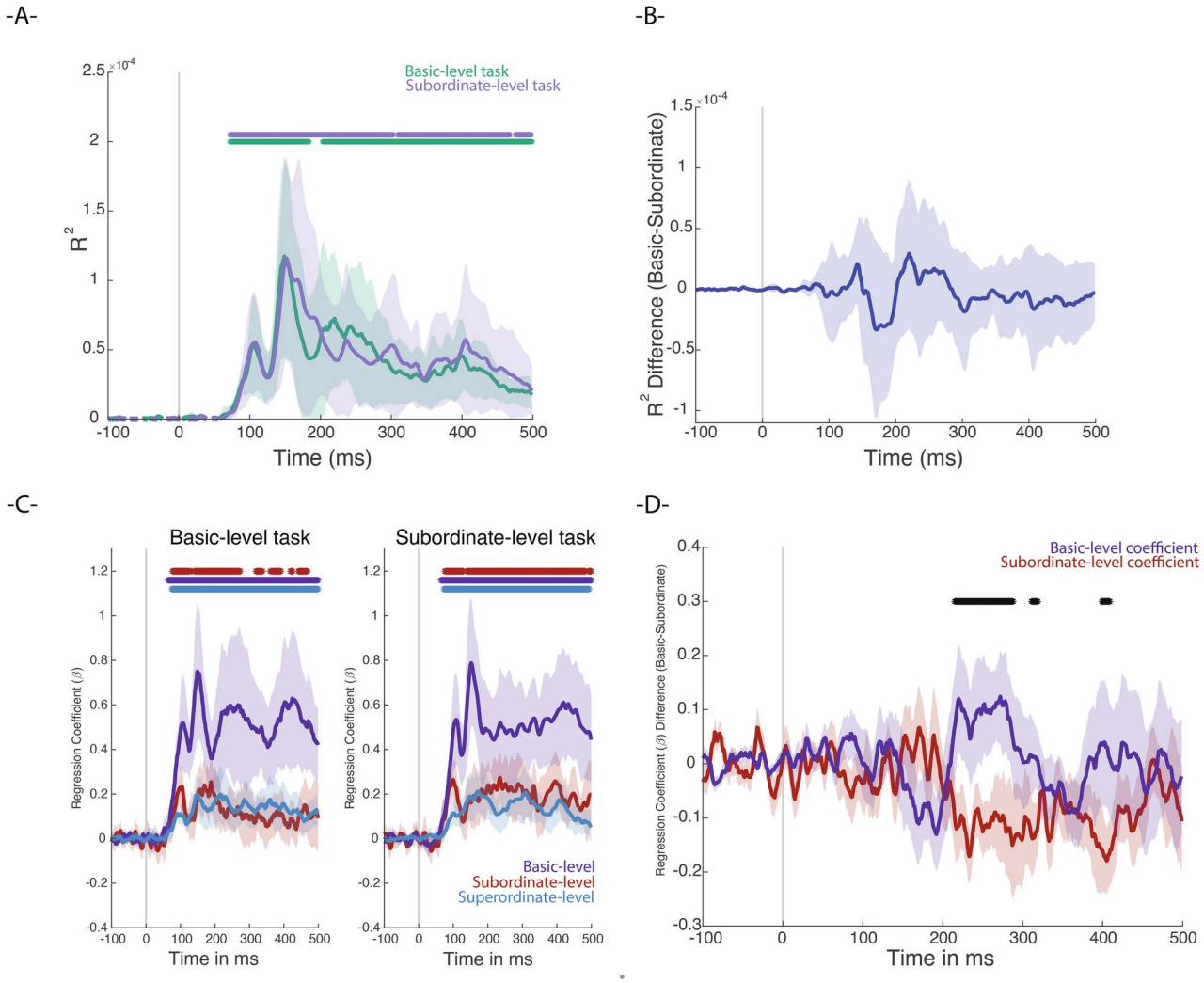

Fig. 2. (**A**) R^2 values for basic- and subordinate-level tasks over time. (**B**) Average differences in R^2 between basic- and subordinate-level tasks. (**C**) Regression coefficients for each of the three orthogonalized category-level models for each of the two tasks. (**D**) Regression coefficient differences between tasks for basic- and subordinate-level coefficients. For each plot, the shaded area indicates 95% confidence intervals, and markers indicate time points that are statistically above baseline (**A**-**C**) or pairwise differences (**D**).

$t(13) = 4.45$, $p = 0.0003$), as well as the superordinate (0.77 versus 0.21, $t(13) = 4.92$, $p = 0.0001$). There was no significant difference between subordinate and superordinate models $t(13) = 1.98$, $p < 0.05$, ns after Bonferroni.

correction). We found no significant effect of task ($F(1,13) < 1$) nor any interaction between task and category model ($F(2,26) < 1$).

When considering the latency of maximum coefficient values, we found no significant effects of task (basic: 169 ms; subordinate: 195 ms, $F(1,13) < 1$), category model (superordinate: 196 ms; basic: 151 ms; subordinate: 199 ms, $F(2,26) < 1$), nor an interaction between these variables ($F(2,26) < 1$).

To assess task-related information usage in a finer manner, we subtracted the coefficients from the subordinate task from those in the basic-level task. For this analysis, we considered only the subordinate- and basic-level coefficients as we did not have a superordinate task. As shown in Fig. 2D, we observed significant task-related differences between 216–318 ms post-image onset, indicating that the neural activity reflected the task-relevant category level during this time period.

Altogether, this analysis demonstrates a neural correlate of the basic-level advantage. However, it does not directly shed light on the genesis of this advantage. To gain better insight, we repeated the same analysis at each electrode.

Electrode-wise multiple regression

We conducted similar regression analyses at each electrode using a 41-ms sliding window (see Methods). Similar to the whole-brain analysis, we examined both the coefficient of determination (R^2) and the regression coefficients for each of the three category models. We also examined the effects in three regions of interest (ROI, see Fig. 1C).

Time-resolved R^2 values for each task and ROI are shown in Fig. 3A and topographically in Fig. 3B. As before, we conducted analyses on the onset, maximum, and latency of maxima. A repeated measures ANOVA on onset with task and ROI as within-subject factors revealed a significant main effect of ROI ($F(2,26) = 3.88$, $p < 0.05$, $ges = 0.95$). Follow-up analysis revealed that anterior onsets (86 ms) were significantly later than posterior (59 ms, $t(13) = 2.59$, $p = 0.01$) and lateral (61 ms, $t(13) = 1.98$, $p = 0.03$) onsets. We observed no significant difference between posterior and lateral ($t(13) < 1$). We observed no main effect of task ($F(1,13) < 1$) nor an interaction between task and ROI ($F(2,26) < 1$). Therefore, category information for all models had a strikingly early onset, this was particularly true over the posterior and lateral scalp electrodes and does not depend on the observer's task.

When considering the maximum R^2 values across ROI and task, we observed a significant main effect of ROI ($F(2,26) = 27.5$, $p = 3.8e\text{-}7$, $ges = 0.99$). Follow-up analysis revealed that maximum R^2 values were larger over posterior electrodes than lateral ($t(13) = 4.8$, $p = 0.0002$) and anterior ($t(13) = 5.66$, $p = 3.9e\text{-}5$) and that lateral values were higher than anterior ($t(13) = 4.33$, $p = 0.0004$). We observed no significant effect of task ($F(1,13) < 1$) or a significant interaction between task and ROI ($F(2,26) < 1$). Thus, category information at each of the hierarchical levels is maximal over posterior electrodes and is reduced as one moves across the scalp in the anterior direction. Finally, we examined the latency of maximum R^2 values across ROI and task. We found no significant effects of either ROI (anterior: 332 ms; lateral: 261 ms; posterior: 149 ms, $F(2,26) < 1$) or task (basic: 260 ms; subordinate: 276 ms, $F(1,13) < 1$), nor a significant interaction between them ($F(2,26) < 1$). Altogether, this analysis has revealed that category information first emerged in posterior electrodes, that there was a gradient of category information that increased over the posterior portion of the scalp, but that the task did not significantly modulate these effects.

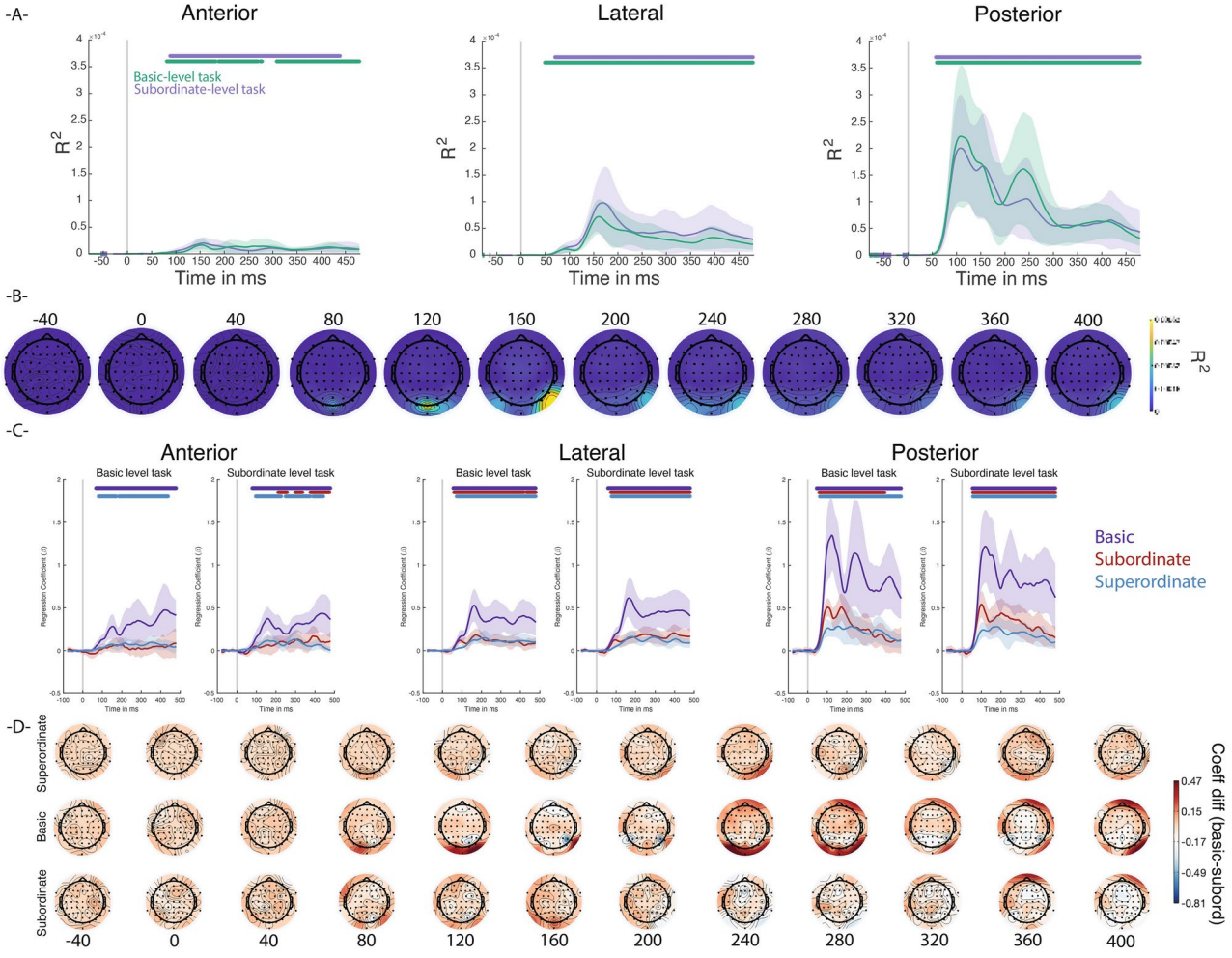

Fig. 3. (**A**) R^2 values over time for basic- and subordinate-level tasks in each of the three regions of interest. Shaded regions indicate 95% confidence intervals, and markers indicate statistical significance. (**B**) Scalp topography of R^2 values. (**C**) Regression coefficients for each of the three orthogonalized category-level models for each of the two tasks in each of the three regions of interest. Shaded regions indicate 95% confidence intervals, and markers indicate statistical significance. (**D**) Scalp topography of regression coefficient differences across tasks.

	Posterior	Lateral	Anterior
Superordinate	0.35	0.19	0.14
Basic	1.54	0.64	0.47
Subordinate	0.60	0.24	0.19

Table 1. Maximum regression coefficient values for each category model and ROI.

We will now turn our attention to the regression coefficients. The results are shown in Fig. 3C. As with R^2, we conducted analyses on the onset, maximum, and latency of maxima. We conducted a repeated-measures ANOVA on onset with task, ROI, and category model as within-subjects factors. We found no significant main effects or interactions. Considering the maximum coefficient values, we observed a significant main effect of ROI ($F(2,26) = 50.0$, $p = 1.2e\text{-}9$, $ges = 0.99$). Follow-up analysis revealed that coefficient values were higher over posterior electrodes than anterior (0.83 versus 0.27, $t(13) = 7.87$, $p = 1.3e\text{-}6$) or lateral (0.83 versus 0.36, $t(13) = 6.86$, $p = 5.7e\text{-}6$). Finally, coefficient values were higher over lateral electrodes than anterior ($t(13) = 2.74$, $p = 0.008$). Furthermore, we observed a significant main effect of category model ($F(2,26) = 60.06$, $p = 1.8e\text{-}10$, $ges = 0.99$). This effect was driven by larger coefficients for the basic-level model compared to the subordinate (0.77 versus 0.30, $t(13) = 6.71$, $p = 7.2e\text{-}6$) and superordinate (0.77 versus 0.21, $t(13) = 8.15$, $p = 9.1e\text{-}7$), as well as larger coefficients for the subordinate level compared to superordinate ($t(13) = 5.87$, $p = 2.8e\text{-}5$). We observed no significant main effect of task ($F(1,13) < 1$), nor an interaction between task and category model ($F(2,26) < 1$), or between task and ROI ($F(2,26) < 1$). However, the ROI and category model interaction was significant ($F(4,52) = 22.05$, $p = 1.1e\text{-}10$, $ges = 0.98$). As shown in Table 1 and Fig. 3C, this was driven by higher basic-level coefficients over posterior electrodes. Table 1lists the maximum coefficient values for each ROI and category model. The values for the superordinate category level were relatively stable across ROIs, while the values for the basic- and subordinate category levels were markedly higher in the posterior and lateral ROIs, consistent with previous EEG work using decoding methods[36]and evocative of the flow of category information across the ventral visual stream, as illustrated by MEG-fMRI fusion[46]. The three-way interaction between task, ROI, and category model was not significant ($F(4,52) < 1$).

We examined the latency of the maximum coefficient values in a similar way. We observed a significant main effect of ROI ($F(2,26) = 11.28$, $p = 0.0003$, $ges = 0.95$). Post-hoc analysis revealed that this effect was driven by earlier latency over the posterior electrodes (149 ms) than lateral (261 ms, $t(13) = 3.32$, $p = 0.003$) or anterior electrodes (332 ms, $t(13) = 3.82$, $p = 0.001$). The difference between lateral and anterior latencies was not statistically significant after correcting for multiple comparisons ($t(13) = 2.14$, $p = 0.03$). No other main effects or interactions were statistically significant. Therefore, regression coefficients were largest for the basic-level model and larger and earlier over more posterior electrodes.

We conducted an exploratory analysis of task differences by subtracting regression coefficient values from the subordinate-level task from those from the basic-level task. The scalp topographies are shown in Fig. 3D. Interestingly, we found adjacent electrodes with different patterns of basic-level regression coefficients over occipitotemporal electrodes between 120–200 ms after stimulus onset. This suggests that the different tasks may engage different neural populations over a similar time course.

Discussion

In most circumstances, human observers spontaneously classify objects at a mid-level of specificity, known as the basic-[6]or entry-level[7]. Despite the robust nature of this effect, little has been known about how the brain organizes itself around this cognitive preference. This work aimed to establish the time course and scalp topography of the basic-level effect for objects, controlling for previously confounding variables.

Although observers were similarly accurate in detecting category repeats at both the basic- and subordinate levels, we found that the basic-level model dominated the multiple regression analyses regarding earlier onset (whole brain partial R^2) and magnitude of effects (regression coefficients). These results agree with what is known about the behavioral[6]and neural[16] precedence of the basic level for categorization.

In this experiment, observers engaged with basic-level and subordinate-level classification in different recording sessions. Task-related differences were not evident in the first 200 ms of post-stimulus processing but rather emerged between 200–300 ms after stimulus onset. This result aligns with previous results that link abstract categorization to this time window[25,28,33], and the correlation time course with reaction times[37]. This may also align with hierarchical models of visual processing that posit low-level feature analysis (invariant to task) is followed by task-specific feature analysis[47]

When examining the onset and magnitude of R^2across ROI, we found earlier effects across posterior electrodes than other ROIs, and a progression from posterior to anterior across the scalp. We also found larger regression coefficients in the posterior ROI. These could imply a feedforward mechanism of category formation[48]. However, a strict feedforward account does not necessarily explain the stronger and earlier basic-level grouping compared to subordinate. Previous fMRI work has demonstrated that subordinate-level grouping was observed in this stimulus set in early visual cortex[16], but we did not observe earlier subordinate-level grouping. Instead, the early usage of basic-level information, even when observers engaged in the subordinate-level task, suggests automatic processing at the basic level[22]. This possibility is strengthened by the exploratory observation that basic-level information was present simultaneously with subordinate-level in different neural populations when observers engaged in the subordinate-level task (see Fig. 3D).

Our study exclusively examined large, inanimate objects. While there is real-world size variability across objects in our dataset (a cargo ship is larger than a piano), all objects were chosen to require at least two human hands for interaction. Furthermore, the objects in the current study were removed from the naturalistic backgrounds and placed on non-meaningful 1/f noise backgrounds. This removed any low-level features potentially correlated with an object's presence, such as the blue sky behind an airplane. Some of the stronger subordinate- and exemplar-level grouping observed in previous studies[49]may be attributed to including these backgrounds because scenes and objects share strong contextual correlations[50–52]. Finally, many extant studies include few exemplars per category[27,28,49]. By including 40 exemplars per subordinate-level category, we better reflect each subordinate-level category's natural variability, allowing us to better generalize the category concept. Any of the above factors could have resulted in the unexpectedly small effects of subordinate-level grouping compared to previous studies.

Taken together, these results clearly show the saliency of the basic level for categorization, starting very early after image onset and even when observers were asked to categorize images at the subordinate level. As categorization is a task that grounds high-level conceptual systems with the sensory systems that support them, these results align with intellectual traditions that see categorization as inexorably linked to perception[2]rather than encapsulated from it[53]. Further, these results align with previous research showing that object categorization is automatic and obligatory[22].

In this study, we found little contribution of the superordinate level of categorization (transportation, musical instruments, and furniture). At first glance, this contradicts some reaction time results showing rapid responses at the superordinate level[54]. However, superordinate category verification may be easy because members of different superordinate categories differ on many features, and affirming just one of these differences may be diagnostic for the task[55]. It has also been argued that the superordinate-level detection advantage disappears when low-level feature similarity is accounted for, as we have done here[56]. Furthermore, behavioral evidence demonstrates that while basic-level categorization is automatic, superordinate-level categorization seems to be inferred from the basic levels[6,22,44]. Developmental evidence supports this view: children learn superordinate-level categories last and use them least frequently[6,43], and the acquisition of superordinate-level concepts is more closely tied to language acquisition than perceptual development[57]. Finally, neural evidence also demonstrates that superordinate-level categories group less coherently within object-selective cortex[16], and are distributed along a broader spatial extent of cortex compared with basic-level categories[58]. Finally, although expertise can shift language use to the subordinate[11], we no studies report increased superordinate label use as a function of learning or other experience in healthy populations. Given the consistency of these findings against the importance of the superordinate level category, we opted not to include a superordinate-level task in the design. However, it may be the case that engaging with the superordinate level would increase the utility of superordinate features, so future work should examine the extent to which attending to superordinate-level membership may change neural processing.

There are multiple theoretical accounts of the basic-level superiority effect. Most theorists agree that this mid-level specificity best achieves the competing aims of maximizing within-category similarity and minimizing between-category similarity[6,59,60]. However, there is less consensus on the origin of this grouping. Early theories indicated that items in the same basic-level category might cluster in terms of their physical features[61]. However, this fell out of favor when object classification turned out to be a non-trivial problem for computer vision (Chihuahuas and Dalmatians are both *dogs*, despite their physical dissimilarities). Others have noted that basic-level categories might increase the efficiency of using and communicating about categories[62], for example, by assigning shorter words for basic-level concepts. Alternatively, basic-level concepts might be the most efficient to search in memory[63] because they minimize the feature overlap between categories while maximizing the feature overlap within categories. All theories agree that the basic level is a tradeoff between detail and diagnosticity. That said, there are very few predictions that these accounts would make that are directly testable with the data from the current experiment.

We observed very few differences in the latency of effects across conditions. In part, the temporal smearing resulting from the sliding window in the electrode-wise analyses may have blurred any possible small effect. In contrast, the whole brain analysis might not have been sensitive to small representational differences across electrodes. A study using fMRI-M/EEG fusion methods[64] may be better able to adjudicate the question of the relative timing of the three category levels.

Finally, categorical perception is predicted by both prototype[65]and boundary-based models[66]. In a prototype account, object representations are compared to a central tendency or prototype. Category boundary effects emerge because items on different sides of a category boundary have a shorter representational distance to one prototype than another. By contrast, boundary accounts emphasize the features that would include an item in the category, irrespective of its position to a central category tendency. While we cannot comment on these two accounts with the present data, a future experiment might examine basic-level supremacy in objects nearer and farther from a central category tendency. A prototype account would predict stronger effects in the near items, while a boundary account would predict stronger effects in the far items.

The present experiment demonstrates a temporal neural correlate of the basic-level supremacy effect. Namely, it is the first and most robust category representation to emerge, and it is only subtly modulated by task demands. These results emphasize the primacy of the basic level for object categorization and provide additional evidence for its automatic nature.

Materials and methods

Participants

Ethical approval was obtained from the Bates College Internal Review Board, written informed consent was obtained from all participants, and the experiment was conducted per the guidelines of this board. 16

participants (ages 18–22, mean age: 19.54, 9 female) from the Bates College community volunteered for this experiment. This sample size was chosen based on previous fMRI work with this image set[16]and is similar to other work that employs regression analysis on EEG[36]. Due to recording errors in two sessions, two participants were excluded from the analysis. Each participant was compensated for their time with a $60 gift card or course credit. Participants provided informed consent and were screened for overall acuity via a standard ETCRS eye chart and for color vision via the Ishihara test. Each participant completed two recording sessions with a median of seven days of separation (range: 4 to 48).

Stimuli

The object stimuli in this experiment consisted of 1080 photographs from a previous study[16]. This image set consists of a three-tiered taxonomy with three superordinate-level categories (conveyances, musical instruments, and furniture). We selected three basic-level categories for each of the superordinate-level categories. For example, *cars*, *airplanes*, and *ships*were the three basic categories of conveyances. These were chosen as non-animate categories with relatively large real-world sizes to avoid known neural differences across these dimensions[40,41]. Finally, three subordinate-level categories were chosen within each of the nine basic-level categories (e.g., *sedan*, *sports car*, and *station wagon*as types of cars). Thus, the set consists of 27 subordinate-level categories with 40 image exemplars per category for 1080 total images. Each object was segmented from its natural background and placed on a colorful 1/f noise background. This noise emulates the spectral properties of natural scenes[67]to ensure that EEG response differences were due to the object rather than its contextually related background[51,52]. Further, as objects differed in aspect ratio, the noise background ensured a constant spatial extent of retinal stimulation in each trial. For more information about dataset creation, see[16]. See example images in Fig. 1A and Supplementary Materials for all category names.

Design

Participants completed two recording sessions. In each, they were instructed to perform a categorical one-back task, pressing a key when images from the same category were repeated consecutively. For example, a biplane followed by an airliner would be a valid repeat at the basic level, while subordinate-level category repeats required the repetition of two different exemplars of (for example) biplanes. In this way, the tasks forced observers to classify objects at a certain level of specificity and maintain this category representation in working memory across repeats. Participants attended to the subordinate-level category in one recording session and the basic-level category in the other. The task of each recording session was counterbalanced across participants. To equate the difficulty and attentional demands across both tasks, both sessions had an equal number of repeats (N = 108). In both cases, participants completed 27 blocks of 40 trials.

Procedure

The experiment was conducted in a dimly lit recording chamber. Participants were seated approximately 60 cm from a 27″ LCD monitor (ASUS VG248Q, resolution: 1920 × 1080 at 100 Hz). While the EEG electrodes were placed on the participant's scalp, the participant viewed a slideshow presentation that explained the hierarchical category structure of the experiment and showed visual examples of members of each subordinate-level category. This ensured that participants understood some of the sometimes subtle differences between subordinate-level categories within each basic-level category. These sample exemplars were not shown in the main experiment.

The experiment consisted of 27 runs of 40 images each. In each run, a black fixation square (approximately 0.3° of visual angle) appeared for a variable duration (sampled from N(300 ms, 30 ms)), followed by an image for 250 ms. Participants were instructed to press the space bar if two consecutive images belonged to the same category as the session's target category level (basic or subordinate). For example, two successive guitars when performing the basic-level task or two consecutive Stratocaster guitars when performing the subordinate-level task. Participants were given up to 950 ms to record their responses. When participants correctly identified category repeats, they received positive feedback ("Correct!" printed on the screen for 500 ms). Negative feedback was provided if a participant missed a repeat or falsely identified a repeat ("Incorrect" printed on screen for 500 ms). No feedback was provided for correct rejections. Thus, this experiment's approximate interstimulus interval (ISI) was 1750 ms, and the intertrial interval was ~ 2000 ms. Participants were allowed to take a self-paced break at the end of each run. They were otherwise asked to remain as still as possible and to minimize movement during the runs.

EEG recording

EEG was recorded with 64 Ag–AgCl active electrodes based on the international 10–20 system. EEG signals were amplified with Brain Products' ActiCHamp system and digitized at 1000 Hz using PyCorder v1.0.9. Impedance levels for each electrode were at or below 15 kΩ before data collection. EEG was referenced online to electrode Fpz and then re-referenced offline to the average of all electrodes. Two electrodes were placed at the bottom and outer canthi of the right eye to detect eye movements and blinks. These were linked to a reference on the right mastoid bone. We time-locked EEG signals to stimulus presentation through a photodiode attached to the bottom left corner of the monitor and obscured from the participant's view.

EEG preprocessing

EEG data were pre-processed with EEGLAB[68]. Raw EEG data were bandpass filtered with a finite impulse response filter with a half-amplitude cutoff of 0.1 Hz and 50 Hz and a 12 dB/octave roll-off. Data were epoched to preserve signals 100 ms before each trial, including 500 ms of stimulus-driven response. Eyeblink artifacts were identified and corrected via independent components analysis. We examined each trial and electrode for artifacts (values larger than 100 μV or smaller than −100 μV). For trials with three or fewer artifactual electrodes,

we re-defined each bad electrode's voltage as its neighbors' average voltage. We omitted trials with more than three bad electrodes from further analysis (median: 7.3 trials omitted, range: 1–61 trials).

Regression methods

To estimate the amount of category information available in the EEG signals at each of the three category levels at each point in time, we adopted a multiple regression approach. Here, we used representational dissimilarity matrices (RDMs[69],) that defined category membership at each level to predict an RDM reflecting neural variability across the experiment. Both whole-brain and electrode-wise regression analyses are explained below and visually in Fig. 1C. Regression analyses were conducted on each participant individually and then averaged.

Model RDMs

We created three 1080 × 1080 model RDMs, reflecting superordinate, basic, and subordinate-level category membership. Due to the hierarchical nature of category membership (images within the same subordinate category also share basic- and superordinate-level membership), we orthogonalized the RDMs to avoid multicollinearity issues. To orthogonalize the representational spaces, we employed linear regression analyses wherein the subordinate RDM was regressed against both the superordinate and basic RDMs, and the basic RDM was regressed against the superordinate RDM. The residuals from these regressions were reshaped back into matrix form to yield orthogonalized RDMs for the basic and subordinate levels. The residuals represent the variance in the lower-level RDMs not explained by the higher-level RDMs. For example, the orthogonalized subordinate RDM represents subordinate-level category information not shared with the basic- or superordinate level. As shown in Fig. 1B, the orthogonalized RDMs emphasize contrasts between a given level and its "parent" level by assigning very low distances within the given level and the highest distances for categories within the next higher level.

Neural RDMs

To employ the model RDMs to predict neural activity, we created two different types of neural RDMs: whole-brain RDMs that reflected the overall patterns of voltage across the scalp and electrode-wise RDMs that examined patterns of voltage at each electrode during a small sliding window of time. To create whole-brain RDMs, we extracted the voltage values for all electrodes across all 1080 trials at each time point. We created a 1080 × 1080 RDM from this array using the Euclidean distance metric. To create RDMs at each electrode, at each time point from 80 ms before stimulus onset to 480 ms after, and at each of the 64 electrodes, we used a 41-ms sliding window (20 ms before through 20 ms after each time point) to extract a 1080-trial by a 41-ms array. The temporal window size was chosen from previous experiments[36,70,71]. This array was transformed into a 1080 × 1080 RDM using the Euclidean distance metric. Thus, separate regression analyses were performed at each electrode and at each time point between 80 ms prior to stimulus onset and 480 ms after stimulus onset. From the set of 64 electrodes, we defined three regions of interest: posterior (Oz, PO7, PO3, POz, PO8, PO4, Iz), lateral (P1, P3, P5, P7, CP1, CP3, CP5, TP7, TP9 P2, P4, P6, P8, CP2, CP4, CP6, TP8, TP10), and anterior (Fp2, AF7. AF3, AFz, AF4, AF8, F1, F3, F5. F7, Fz, F2, F4, F6, F8), see Fig. 1C for a visual map of these ROIs.

Statistical analysis

In each regression analysis, we collated the lower triangles of the three vectorized model RDMs into a 3 × 582,660 matrix of predictors. Then, in each time point (whole brain) or time point and electrode (electrode-wise), we extracted a neural RDM (lower triangle). We used multiple regression to predict the neural RDM with the model RDMs. We saved both regression coefficients (β) and R^2 in each analysis.

We examined three primary dependent measures for both coefficients (β) and R^2 for each time-resolved multiple regression analysis: the maximum value in each condition (establishing the amount of category information), the latency when this maximum was reached (establishing when the brain had peak information), and the onset time (establishing the start of category-specific processing), defined as the latency when values exceeded the group 95% confidence interval established during the pre-stimulus baseline. To increase the signal-to-noise ratio of these measures, we employed a jackknife approach, iteratively computing the mean in 13 of the 14 participants. Accordingly, all t- and F- values have been corrected by dividing by (n-1) and $(n-1)^2$, respectively[72].

To assess the statistical significance of a given time point while controlling for multiple comparisons, we employed permutation-based cluster statistics across adjacent time points, as suggested by[73]. Specifically, we generated empirical null distributions from 10,000 permutations. Each permutation consisted of randomly sampled time points within the pre-stimulus baseline. We employed cluster-based correction for multiple comparisons, wherein clusters of temporally contiguous significant points were identified. The sum of t-statistics within each cluster served as the cluster-level statistic, with significance determined based on a threshold set at the 95th percentile of the permutation-derived null distribution.

Data availability

The datasets generated during and/or analyzed during the current study are available in the OSF repository, https://osf.io/x3yvd/.

Received: 9 April 2024; Accepted: 19 November 2024
Published online: 02 January 2025

References

1. Thorpe, S., Fize, D. & Marlot, C. Speed of processing in the human visual system. *Nature* **381**, 520–522 (1996).
2. Bruner, J. S. On perceptual readiness. *Psychol. Rev.* **64**, 123–152 (1957).
3. Murphy, G. L. *The Big Book of Concepts*. (MIT Press, 2004).
4. Miller, G. A. WordNet: a lexical database for English. *Commun ACM* **38**, 39–41 (1995).
5. Brown, R. How shall a thing be called. *Psychol. Rev.* **65**, 14–21 (1958).
6. Rosch, E., Mervis, C. B., Gray, W. D., Johnson, D. M. & Boyes-Braem, P. Basic objects in natural categories. *Cognit. Psychol.* **8**, 382–439 (1976).
7. Jolicoeur, P., Gluck, M. A. & Kosslyn, S. M. Pictures and names: making the connection. *Cognit. Psychol.* **16**, 243–275 (1984).
8. Johnson, K. E., Scott, P. & Mervis, C. B. Development of Children's Understanding of Basic-Subordinate Inclusion Relations. *Dev. Psychol.* **33**, 745–763 (1997).
9. Mervis, C. B. Acquisition of a lexicon. *Contemp. Educ. Psychol.* **8**, 210–236 (1983).
10. Mack, M. L., Wong, A.C.-N., Gauthier, I., Tanaka, J. W. & Palmeri, T. J. Time course of visual object categorization: Fastest does not necessarily mean first. *Vision Res.* **49**, 1961–1968 (2009).
11. Tanaka, J. W. & Taylor, M. Object categories and expertise: Is the basic level in the eye of the beholder?. *Cognit. Psychol.* **23**, 457–482 (1991).
12. Grill-Spector, K. The neural basis of object perception. *Curr. Opin. Neurobiol.* **13**, 159–166 (2003).
13. Malach, R. et al. Object-related activity revealed by functional magnetic resonance imaging in human occipital cortex. *Proc. Natl. Acad. Sci. U. S. A.* **92**, 8135–8139 (1995).
14. Carlson, T. A., Schrater, P. & He, S. Patterns of Activity in the Categorical Representations of Objects. *J. Cogn. Neurosci.* **15**, 704–717 (2003).
15. Haxby, J. V. et al. Distributed and Overlapping Representations of Faces and Objects in Ventral Temporal Cortex. *Science* **293**, 2425–2430 (2001).
16. Iordan, M. C., Greene, M. R., Beck, D. M. & Fei-Fei, L. Basic Level Category Structure Emerges Gradually across Human Ventral Visual Cortex. *J. Cogn. Neurosci.* **27**, 1427–1446 (2015).
17. O'Toole, A. J., Jiang, F., Abdi, H. & Haxby, J. V. Partially Distributed Representations of Objects and Faces in Ventral Temporal Cortex. *J. Cogn. Neurosci.* **17**, 580–590 (2005).
18. Stansbury, D. E., Naselaris, T. & Gallant, J. L. Natural scene statistics account for the representation of scene categories in human visual cortex. *Neuron* **79**, 1025–1034 (2013).
19. Potter, M. C. Meaning in visual search. *Science* **187**, 965–966 (1975).
20. Potter, M. C., Wyble, B., Hagmann, C. E. & McCourt, E. S. Detecting meaning in RSVP at 13 ms per picture. *Atten. Percept. Psychophys.* 1–10 (2014) https://doi.org/10.3758/s13414-013-0605-z.
21. VanRullen, R. & Thorpe, S. J. The time course of visual processing: From early perception to decision-making. *J. Cogn. Neurosci.* **13**, 454–461 (2001).
22. Greene, M. R. & Fei-Fei, L. Visual categorization is automatic and obligatory: Evidence from Stroop-like paradigm. *J. Vis.* **14**, 14–14 (2014).
23. Mathis, K. M. Semantic interference from objects both in and out of a scene context. *J. Exp. Psychol. Learn. Mem. Cogn.* **28**, 171–182 (2002).
24. Clarke, A., Devereux, B. J. & Tyler, L. K. Oscillatory Dynamics of Perceptual to Conceptual Transformations in the Ventral Visual Pathway. *J. Cogn. Neurosci.* **30**, 1590–1605 (2018).
25. Bankson, B. B., Hebart, M. N., Groen, I. I. A. & Baker, C. I. The temporal evolution of conceptual object representations revealed through models of behavior, semantics and deep neural networks. *NeuroImage* **178**, 172–182 (2018).
26. Clarke, A., Taylor, K. I., Devereux, B., Randall, B. & Tyler, L. K. From perception to conception: how meaningful objects are processed over time. *Cereb. Cortex N. Y. N* **1991**(23), 187–197 (2013).
27. Iamshchinina, P., Karapetian, A., Kaiser, D. & Cichy, R. M. Resolving the time course of visual and auditory object categorization. *J. Neurophysiol.* **127**, 1622–1628 (2022).
28. Carlson, T., Tovar, D. A., Alink, A. & Kriegeskorte, N. Representational dynamics of object vision: The first 1000 ms. *J. Vis.* **13**, 1–1 (2013).
29. Chan, A. M. et al. First-Pass Selectivity for Semantic Categories in Human Anteroventral Temporal Lobe. *J. Neurosci.* **31**, 18119–18129 (2011).
30. Clarke, A., Taylor, K. I. & Tyler, L. K. The Evolution of Meaning: Spatio-temporal Dynamics of Visual Object Recognition. *J. Cogn. Neurosci.* **23**, 1887–1899 (2011).
31. Clarke, A. & Tyler, L. K. Understanding What We See: How We Derive Meaning From Vision. *Trends Cogn. Sci.* **19**, 677–687 (2015).
32. Cichy, R. M., Kriegeskorte, N., Jozwik, K. M., van den Bosch, J. J. F. & Charest, I. The spatiotemporal neural dynamics underlying perceived similarity for real-world objects. *NeuroImage* **194**, 12–24 (2019).
33. Cichy, R. M., Pantazis, D. & Oliva, A. Resolving human object recognition in space and time. *Nat. Neurosci.* **17**, 455–462 (2014).
34. Cichy, R. M., Khosla, A., Pantazis, D., Torralba, A. & Oliva, A. Comparison of deep neural networks to spatio-temporal cortical dynamics of human visual object recognition reveals hierarchical correspondence. *Sci. Rep.* **6**, 27755 (2016).
35. Isik, L., Meyers, E. M., Leibo, J. Z. & Poggio, T. The dynamics of invariant object recognition in the human visual system. *J. Neurophysiol.* **111**, 91–102 (2014).
36. Greene, M. R. & Hansen, B. C. Disentangling the Independent Contributions of Visual and Conceptual Features to the Spatiotemporal Dynamics of Scene Categorization. *J. Neurosci.* **40**, 5283–5299 (2020).
37. Ritchie, J. B., Tovar, D. A. & Carlson, T. A. Emerging Object Representations in the Visual System Predict Reaction Times for Categorization. *PLOS Comput. Biol.* **11**, e1004316 (2015).
38. Wardle, S. G., Kriegeskorte, N., Grootswagers, T., Khaligh-Razavi, S.-M. & Carlson, T. A. Perceptual similarity of visual patterns predicts dynamic neural activation patterns measured with MEG. *NeuroImage* **132**, 59–70 (2016).
39. Carlson, T. A., Hogendoorn, H., Kanai, R., Mesik, J. & Turret, J. High temporal resolution decoding of object position and category. *J. Vis.* **11**, 9 (2011).
40. Connolly, A. C. et al. The Representation of Biological Classes in the Human Brain. *J. Neurosci.* **32**, 2608–2618 (2012).
41. Konkle, T. & Caramazza, A. Tripartite Organization of the Ventral Stream by Animacy and Object Size. *J. Neurosci.* **33**, 10235–10242 (2013).
42. Wisniewski, E. J. & Murphy, G. L. Superordinate and basic category names in discourse: A textual analysis. *Discourse Process.* **12**, 245–261 (1989).
43. Singer-Freeman, K. E. & Bauer, P. J. Sorting out language and level: examining the relation between productive vocabulary and category differentiation. *First Lang.* **17**, 241–270 (1997).
44. Potter, M. C. & Hagemann, C. Banana or fruit? Detection and recognition across categorical levels in RSVP. *Psychon. Bull. Rev.* **22**, 578–585 (2014).
45. Clarke, A., Devereux, B. J., Randall, B. & Tyler, L. K. Predicting the Time Course of Individual Objects with MEG. *Cereb. Cortex* **25**, 3602–3612 (2015).
46. Cichy, R. M., Pantazis, D. & Oliva, A. Similarity-Based Fusion of MEG and fMRI Reveals Spatio-Temporal Dynamics in Human Cortex During Visual Object Recognition. *Cereb. Cortex* **26**, 3563–3579 (2016).

47. Kravitz, D. J., Saleem, K. S., Baker, C. I., Ungerleider, L. G. & Mishkin, M. The ventral visual pathway: an expanded neural framework for the processing of object quality. *Trends Cogn. Sci.* **17**, 26–49 (2013).
48. Serre, T., Oliva, A. & Poggio, T. A feedforward architecture accounts for rapid categorization. *Proc. Natl. Acad. Sci.* **104**, 6424–6429 (2007).
49. Cichy, R. M., Khosla, A., Pantazis, D. & Oliva, A. Dynamics of scene representations in the human brain revealed by magnetoencephalography and deep neural networks. *NeuroImage* **153**, 346–358 (2017).
50. Bar, M. & Aminoff, E. Cortical analysis of visual context. *Neuron* **38**, 347–358 (2003).
51. Davenport, J. & Potter, M. C. Scene consistency in object and background perception. *Psychol. Sci.* **15**, 559–564 (2004).
52. Greene, M. R. Statistics of high-level scene context. *Front. Percept. Sci.* **4**, 777 (2013).
53. Firestone, C. & Scholl, B. J. Cognition does not affect perception: Evaluating the evidence for 'top-down' effects. *Behav. Brain Sci.* 1–77 (2015) https://doi.org/10.1017/S0140525X15000965.
54. Macé, M.J.-M., Joubert, O. R., Nespoulous, J.-L. & Fabre-Thorpe, M. The Time-Course of Visual Categorizations: You Spot the Animal Faster than the Bird. *PLoS ONE* **4**, e5927 (2009).
55. Mack, M. L. & Palmeri, T. J. The timing of visual object categorization. *Percept. Sci.* **2**, 165 (2011).
56. Banno, H. & Saiki, J. The Processing Speed of Scene Categorization at Multiple Levels of Description: The Superordinate Advantage Revisited. *Perception* **44**, 269–288 (2015).
57. Horton, M. S. & Markman, E. M. Developmental Differences in the Acquisition of Basic and Superordinate Categories. *Child Dev.* **51**, 708–719 (1980).
58. Bauer, A. & Just, M. A. A brain-based account of "basic-level" concepts. *NeuroImage* **161**, (2017).
59. Murphy, G. & Smith, E. Basic-level superiority in picture categorization. *J. Verbal Learn. Verbal Behav.* **21**, 1–20 (1982).
60. Rosch, E. & Mervis, C. B. Family resemblances: Studies in the internal structure of categories. *Cognit. Psychol.* **7**, 573–605 (1975).
61. Pomerantz, J. R. & Kubovy, M. Perceptual Organization: An Overview. in *Perceptual Organization* (Routledge, 1981).
62. Pothos, E. M. & Chater, N. A simplicity principle in unsupervised human categorization. *Cogn. Sci.* **26**, 303–343 (2002).
63. Gosselin, F. & Schyns, P. G. Why do we SLIP to the basic level? Computational constraints and their implementation. *Psychol. Rev.* **108**, 735–758 (2001).
64. Cichy, R. M. & Oliva, A. A M/EEG-fMRI Fusion Primer: Resolving Human Brain Responses in Space and Time. *Neuron* **107**, 772–781 (2020).
65. Lakoff, G. *Women, Fire, and Dangerous Things: What Categories Reveal about the Mind*. (Univ. of Chicago Press, 2008).
66. Pastore, R. E. Categorical perception: Some psychophysical models. in *Categorical perception: The groundwork of cognition* 29–52 (Cambridge University Press, New York, NY, US, 1987).
67. Field, D. J. Relations between the statistics of natural images and the response properties of cortical cells. *J. Opt. Soc. Am.* **4**, 2379–2394 (1987).
68. Delorme, A. & Makeig, S. EEGLAB: an open source toolbox for analysis of single-trial EEG dynamics including independent component analysis. *J. Neurosci. Methods* **134**, 9–21 (2004).
69. Kriegeskorte, N. et al. Matching Categorical Object Representations in Inferior Temporal Cortex of Man and Monkey. *Neuron* **60**, 1126–1141 (2008).
70. Greene, M. R. & Hansen, B. C. Shared spatiotemporal category representations in biological and artificial deep neural networks. *PLOS Comput. Biol.* **14**, e1006327 (2018).
71. Ramkumar, P., Hansen, B. C., Pannasch, S. & Loschky, L. C. Visual information representation and rapid-scene categorization are simultaneous across cortex: An MEG study. *NeuroImage* **134**, 295–304 (2016).
72. Luck, S. J. *An Introduction to the Event-Related Potential Technique* (The MIT Press, 2014).
73. Maris, E. & Oostenveld, R. Nonparametric statistical testing of EEG- and MEG-data. *J. Neurosci. Methods* **164**, 177–190 (2007).

Acknowledgements
The authors thank Coraline Rinn Iordan for helpful discussions about the manuscript.

Author contributions
M.R.G conceived of the presented idea. Both authors collected and analyzed the data, discussed the results, and contributed to the final manuscript.

Declarations

Competing interests
The authors declare no competing interests.

Additional information
Supplementary Information The online version contains supplementary material available at https://doi.org/10.1038/s41598-024-80546-4.

Correspondence and requests for materials should be addressed to M.R.G.

Reprints and permissions information is available at www.nature.com/reprints.

Publisher's note Springer Nature remains neutral with regard to jurisdictional claims in published maps and institutional affiliations.

Open Access This article is licensed under a Creative Commons Attribution-NonCommercial-NoDerivatives 4.0 International License, which permits any non-commercial use, sharing, distribution and reproduction in any medium or format, as long as you give appropriate credit to the original author(s) and the source, provide a link to the Creative Commons licence, and indicate if you modified the licensed material. You do not have permission under this licence to share adapted material derived from this article or parts of it. The images or other third party material in this article are included in the article's Creative Commons licence, unless indicated otherwise in a credit line to the material. If material is not included in the article's Creative Commons licence and your intended use is not permitted by statutory regulation or exceeds the permitted use, you will need to obtain permission directly from the copyright holder. To view a copy of this licence, visit http://creativecommons.org/licenses/by-nc-nd/4.0/.

© The Author(s) 2025